CHEMISTRY
A European Journal

A Journal of
ChemPubSoc Europe

Accepted Article

Title: Probing the Proton-Coupled Electron Transfer Reactivity of a Cross-Conjugated Cruciform Chromophore by Redox-State Dependent Fluorescence

Authors: Conrad Wagner, Olaf Hübner, Elisabeth Kaifer, and Hans-Jörg Himmel

To be cited as: *Chem. Eur. J.* 10.1002/chem.201900268

Link to VoR: http://dx.doi.org/10.1002/chem.201900268

Supported by
ACES

WILEY-VCH

10.1002/chem.201900268

COMMUNICATION

WILEY-VCH

Probing the Proton-Coupled Electron Transfer Reactivity of a Cross-Conjugated Cruciform Chromophore by Redox-State Dependent Fluorescence

Conrad Wagner, Olaf Hübner, Elisabeth Kaifer, Hans-Jörg Himmel*[a]

Abstract: Proton-coupled electron transfer (PCET) reactions are of great importance in synthetic chemistry and in biology, but the acquisition of kinetic information for these reactions is often difficult. Herein, we report the synthesis of a new PCET reagent, showing redox-state dependent fluorescence, by merging the concept of cross-conjugated cruciform chromophores with the strategy of imposing redox activity and Brønsted basicity to aromatic compounds by substitution with guanidino groups. The compound is isolated and characterized in all stable states – reduced, twofold and fourfold protonated and twofold oxidized – and then applied in PCET reactions, using its redox-state dependent fluorescence signal for kinetic measurements.

Proton-coupled electron transfer (PCET) processes are often key steps in synthetic chemistry and biology,[1-3] as well as atmospheric chemistry.[4] Biology generally uses protonation to adjust the redox potentials in redox-enzymatic reactions. Mechanistic insight in these reactions is not trivial, since several pathways are plausible, even if only one proton and electron are involved.[5-9] Hence proton and electron transfer proceed either simultaneously or subsequently. Then, hydrogen-atom transfer (HAT) processes are possible (especially for nitrogen- or oxygen-centered radicals), for which (in a concerted pathway) proton and electron transfer involve the same orbitals of the two reactants.[10-12] Moreover, PCET can occur from the electronic ground state or from excited states.[13] If more than one proton and electron are transferred, the situation becomes even more complicated and a number of possible intermediates have to be considered. An analysis via NMR or UV/Vis spectroscopy becomes often challenging or impossible, since all involved species contribute to the spectra. In the light of these difficulties, it is highly desirable to use PCET reagents with redox-state dependent fluorescence, allowing facile measurement of the rates of electron transfer in these reactions. However, purely organic reagents with such properties, that are stable in all relevant states (reduced, protonated and oxidized), are almost completely unknown. Very recently, Heiden et al. reported the synthesis of the fluorescent 4,4-difluoro-4-bora-3a,4a-diaza-s-indacene (BODIPY) derivative BoTMG (Scheme 1) with a tetramethylguanidino (TMG) group in the 8-position.[14] Although the BODIPY group reduces the guanidine basicity, the compound can be protonated quantitatively with $HBF_4{\cdot}OEt_2$ to $(BoTMG+H)^+$ (Scheme 1). Protonation reduces the quantum yield for fluorescence (from 17% to 13%). On the other hand, one-electron reduction of BoTMG to the radical monoanion quenches the fluorescence. The reagent enables a reaction sequence (Scheme 1) in which a hydrogen atom is transferred to TEMPO.

In recent years, Guanidino-Functionalized Aromatics (GFAs),[15,16] that combine redox activity with high Brønsted basicity, were established by our group as a new class of PCET reagents and redox-catalysts.[16-18] GFAs are generally readily synthesized in good yield,[16] and represent valuable additions to established PCET reagents such as quinones.[19] By merging the "GFA concept" with the concept of cross-conjugated cruciform fluorophores,[20] we report herein the synthesis of the new chromophore 1,2,4,5-tetrakis(tetramethylguanidino)-3,6-bis-((triisopropylsilyl)-ethynyl)-benzene, **1** (Scheme 1 and Figure 1). Its redox-state dependent fluorescence is used to study the kinetics of PCET reactions.

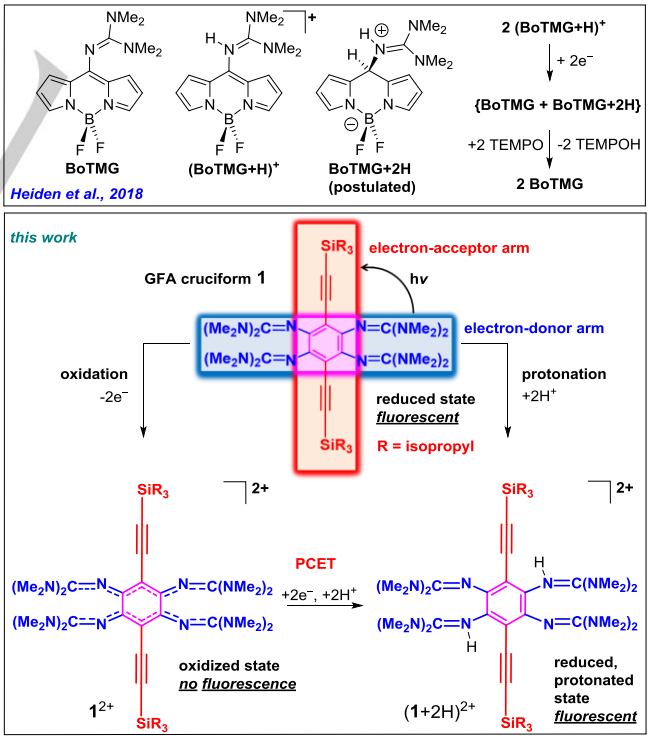

Scheme 1. The fluorescent chromophore BoTMG and its chemistry, reported by Heiden et al., and the first fluorescent redox-active tetrakisguanidine **1** reported in this work.

Bright-yellow **1** is obtained in 43% isolated yield over two steps starting with a benzothiadiazole precursor (see SI for details). It

[a] C. Wagner, Dr. O. Hübner, Dr. E. Kaifer, Prof. H.-J. Himmel,
Anorganisch-Chemisches Institut
Ruprecht-Karls-University of Heidelberg
Im Neuenheimer Feld 270, 69120 Heidelberg
E-mail: hans-jorg.himmel@aci.uni-heidelberg.de

Supporting information for this article is given via a link at the end of the document.

is soluble in less-polar solvents (THF, Et_2O and toluene), but poorly soluble in polar solvents (CH_3CN). Crystals suitable for structural analysis precipitate from an Et_2O solution (Figure 1 and SI).

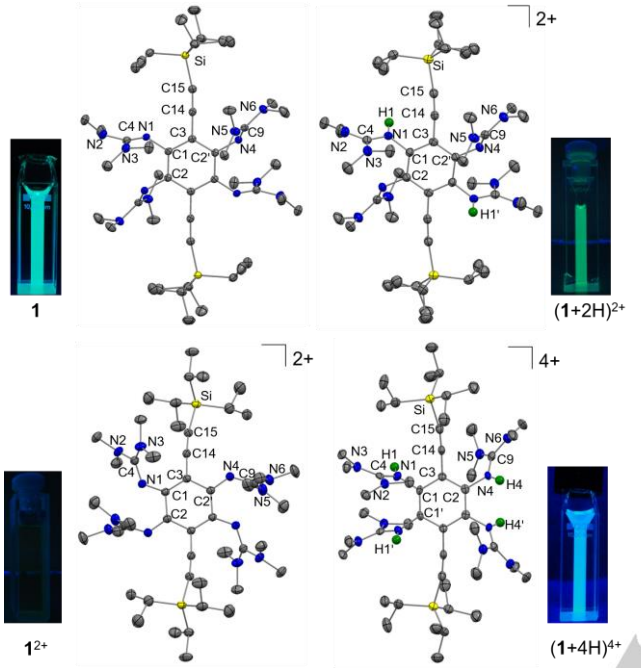

Figure 1. Structures of the new redox-active tetrakisguanidine in all stable charge and protonation states. C-H hydrogens and counterions omitted for clarity. Vibrational ellipsoids drawn at the 50% probability level. Color code: C grey, N blue, Si yellow, H green. Photos of the luminescence (CH_3CN solution for $(\mathbf{1}+4H)^{4+}$, all others THF solutions) under UV light are included.

A broad, intense absorption appears at 433 nm in the UV/Vis spectra of THF solutions (Figure 2). According to TD-DFT calculations (B3LYP/def2-TZVP), this band originates from a pure HOMO → LUMO transition (calculated at 429 nm, Figure 2). While the HOMO is localized on the electron-rich arm of the cruciform (guanidino groups - aromatic ring), the LUMO is predominantly localized on its electron-acceptor arm (π^* of the alkynyl groups - aromatic ring). Hence the lowest-energy electronic transition has charge-transfer character from one arm to the other, as characteristic for cruciform chromophores.

Notably, the compound shows fluorescence, with maximum of emission at 502 nm in THF solution (Figure 3). The Stokes shift measures 3332 cm^{-1} and the quantum yield 18%.

Reaction of **1** with NH_4PF_6 yields the diprotonated compound $(\mathbf{1}+2H)^{2+}$ in an isolated yield of 92%, that crystallizes from a THF solution (Figure 1 and SI). Protonation occurs at the imino N atoms of two guanidino groups in *para*-position to each other, and leads to characteristic structural changes of these groups such as the elongation of the C=N imino bonds. In the UV/Vis spectrum, the lowest-energy band is slightly blue-shifted from 433 nm in **1** to 419 nm in $(\mathbf{1}+2H)^{2+}$ (Figure 3), and exhibits a slightly larger extinction coefficient (10900 $M^{-1}cm^{-1}$ for **1** and 13300 $M^{-1}cm^{-1}$ for $(\mathbf{1}+2H)^{2+}$). The wavelength of the fluorescence maximum is almost unchanged (λ_{em} = 502 nm for **1** and 508 nm for $(\mathbf{1}+2H)^{2+}$), but the quantum yield significantly increases from 18% in **1** to 31% in $(\mathbf{1}+2H)^{2+}$ at room temperature.

Temperature-dependent measurements showed that the fluorescence intensity for $(\mathbf{1}+2H)^{2+}$ rapidly decreases with increasing temperature, and increases at lower temperatures (see Figure 3).

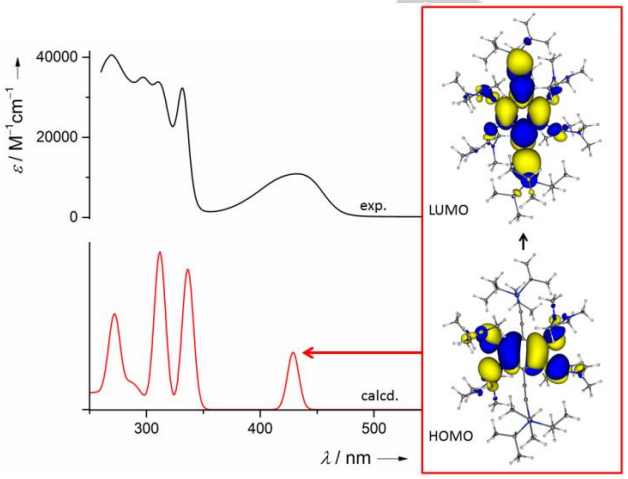

Figure 2. Comparison between the experimental UV/Vis spectrum of **1** in THF and a simulation from TD-DFT (B3LYP/def2-TZVP). The lowest energy band arises from a pure HOMO → LUMO excitation from the donor arm to the acceptor arm (see plots of isodensity surfaces).

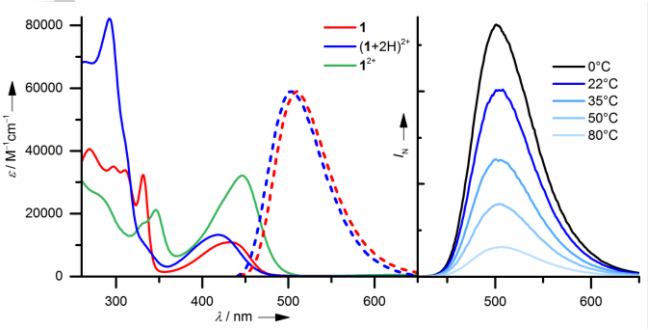

Figure 3. Left: UV/Vis spectra and (normalized) fluorescence spectra (dotted lines) for **1** (λ_{ex} = 433 nm), $(\mathbf{1}+2H)^{2+}$ (λ_{ex} = 417 nm) and $\mathbf{1}^{2+}$ (fluorescence silent) in THF. Right: Temperature dependent emission spectra for $(\mathbf{1}+2H)^{2+}$ in CH_3CN.

Table 1: Comparison between absorption and emission wavelengths (in nm), with ε in $M^{-1}cm^{-1}$ in parenthesis, fluorescence quantum yield Φ and lifetime τ (in ns) for all isolated compounds (in THF solution; $(\mathbf{1}+4H)^{4+}$: in CH_3CN).

Compound	$\lambda_{max,\ abs.}$ (ε)	$\lambda_{max,\ em.}$	Φ	τ
1	332 (32200), 433 (10900)	502	0.18	2.3
$(\mathbf{1}+2H)^{2+}$	293 (82100), 419 (13300)	508	0.31	3.9
$\mathbf{1}^{2+}$	346 (21200), 446 (32100)	-	-	-
$(\mathbf{1}+4H)^{4+}$	279 (47000), 392 (4800)	477	0.33	5.3

Even with an excess of NH_4PF_6, the twofold protonated compound, $(\mathbf{1}+2H)^{2+}$, cannot be protonated further. Protonation of all guanidino groups, leading to $(\mathbf{1}+4H)^{4+}$, is only achieved with a stronger acid such as HCl (see Figure 1 and SI). In

CH_3CN solution, pK_a = 10.43 for HCl and ca. 16 for NH_4^+.[21,22] Therefore, (**1**+4H)$^{4+}$ is not relevant for the PCET reactivity. The quantum yield for fluorescence increases upon protonation (from Φ = 0.18 for **1** to 0.31 for (**1**+2H)$^{2+}$ and 0.33 for (**1**+4H)$^{4+}$), and the fluorescence lifetime also increases (from τ = 2.3 ns for **1** to 3.9 ns for (**1**+2H)$^{2+}$ and 5.3 ns for (**1**+4H)$^{4+}$, see SI).

The cyclic voltammogram (CV) of **1** in CH_2Cl_2 solution (Figure 4) shows a reversible two-electron wave at $E_{1/2}$ = −0.65 V (E_{ox} = −0.60 V) vs. Fc^+/Fc for the redox couple **1**$^{2+}$/**1**, and a one-electron wave at $E_{1/2}$ = +0.65 V (E_{ox} = +0.60 V), that is tentatively assigned to the redox couple **1**$^{\bullet 3+}$/**1**$^{2+}$. As expected, the potential needed for oxidation shifts to higher values upon addition of NH_4PF_6. We tentatively assign oxidation waves at E_{ox} = −0.13 V to oxidation of the (unstable) monoprotonated species, (**1**+H)$^+$, and at E_{ox} = +0.18 V to oxidation of the diprotonated species, (**1**+2H)$^{2+}$. Evidently, the protonated and oxidized molecules are very strong Brønsted acids that immediately transfer their protons to non-oxidized molecules.[23] Consequently, the redox process is not reversible, and the reduction wave remains at E_{red} = −0.75 V (the value for the non-protonated compound).

Chemical oxidation of **1** with 2 equivalents of $FcPF_6$ in CH_3CN affords green **1**$^{2+}$ in 70% isolated yield, that is crystallized by slow diffusion of Et_2O into saturated CH_3CN solutions (Figure 1). Since the HOMO does not involve orbitals of the alkynyl groups, oxidation does not significantly change the wavenumber of the (out-of-phase) ν(C≡C) stretching mode in the IR spectrum (2134 cm^{-1} in **1** and 2137 cm^{-1} in **1**$^{2+}$, see SI). In the UV/Vis spectrum of the oxidized compound, a very strong absorption appears at λ_{max} = 446 nm, being only slightly shifted from that of neutral **1**, but with three times higher extinction coefficient (Figure 3). The similarity of the absorption wavelengths for **1**$^{2+}$ and (**1**+2H)$^{2+}$ hampers the monitoring of PCET reactions by UV/Vis spectroscopy.

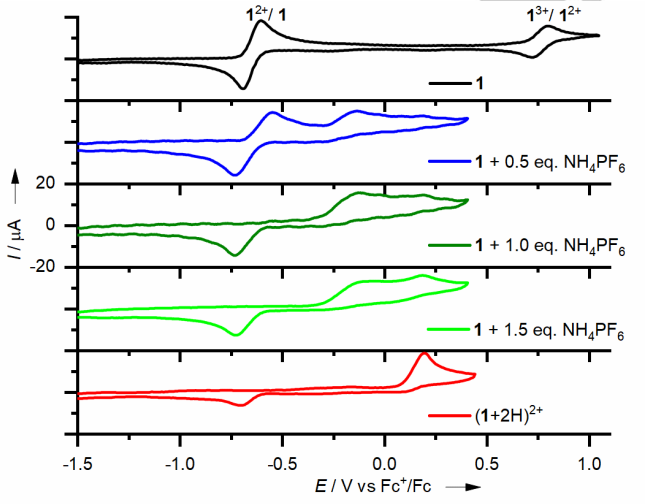

Figure 4. Cyclic voltammogram of **1** (top) in CH_2Cl_2 and (**1**+2H)$^{2+}$ (bottom) in THF. The voltammograms in the middle show the effect of protonation with NH_4PF_6 on the CV curves (THF). Bu_4NPF_6 as supporting electrolyte, scan rate of 100 mV s^{-1}. Potentials are given vs. ferrocenium/ferrocene (Fc^+/Fc).

Most importantly, the fluorescence is completely quenched upon two-electron oxidation. According to DFT calculations (see SI), the HOMO of **1**$^{2+}$ involves primarily orbitals of the alkynyl group (π) and the central C_6 unit, while the LUMO is similar to the HOMO of neutral **1**. Hence the charge-transfer character (from one cruciform arm to the other) of the lowest-energy electronic excitation is now reversed, motivating the distinct change in the optical properties upon oxidation.

Next, the redox-state dependent fluorescence of the new cruciform chromophore **1** is applied in test PCET reactions. The reactions of **1**$^{2+}$ with *p*-methoxy-thiophenol and with 3,5-ditertbutyl-catechol were chosen for this purpose (Scheme 2), since the similar reactions between related (non-fluorescent) redox-active guanidines in their oxidized states proceed fast and quantitatively.[18] First the reactions were followed by NMR spectroscopy. In both cases clean reactions without any byproduct formation were observed. The initial non-fluorescent reaction mixtures turn into fluorescent solutions upon formation of (**1**+2H)$^{2+}$ in the course of the PCET reactions (see photos in Figure 5). The NMR spectra showed that neutral **1** is not formed in the course of the reaction. Hence the fluorescence signal from the solution only arises from (**1**+2H)$^{2+}$. Under the applied conditions (see caption to Figure 5 and SI), 93% disulfide was formed within 260 min. The catechol reaction is slower. A catechol conversion of 92% is obtained after 1400 min reaction time. The absence of signals from intermediate species in the NMR spectra argues for a concerted transfer of electrons and protons (concerted PCET process). The dication (**1**+2H)$^{2+}$ does not react with TEMPO (see SI), in line with the absence of typical hydrogen-atom transfer (HAT) reactivity. Interestingly, the reaction is markedly slower than the similar reaction of the oxidized form of the non-fluorescent redox-active guanidine 1,2,4,5-tetrakis(tetramethylguanidino)-benzene.[18]

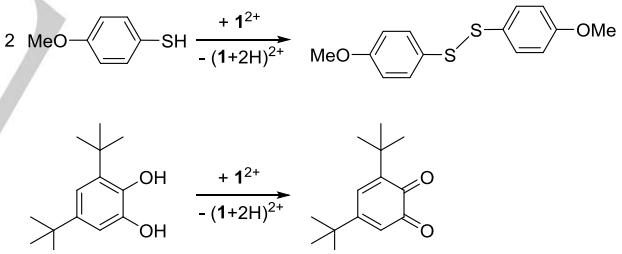

Scheme 2. Test PCET reactions (thiol - disulfide and catechol - benzoquinone) carried out with the new redox-active tetrakisguanidine. The product (**1**+2H)$^{2+}$ is fluorescent, while the reactand **1**$^{2+}$ is non-fluorescent.

According to quantum chemical calculations (B3LYP), the reaction with the catechol is near thermoneutral (ΔH = –7.8 kJ mol^{-1} at 0 K and ΔG = +8.0 kJ mol^{-1} at 298 K, 1 bar, without inclusion of the solvent effect). To assess the practicability of fluorescence measurements for the analysis of the kinetics of PCET reactions, the concentration is decreased by a factor of more than 100 compared to the NMR experiments, with an initial ratio of catechol to **1**$^{2+}$ of 10:1. As expected, in all experiments the fluorescence signal starts to grow upon mixing the two reactants together, signalling formation of fluorescent (**1**+2H)$^{2+}$ from non-fluorescent **1**$^{2+}$. In Figure 6, the normalized fluorescence intensity I_N (for λ_{ex} = 417 nm) is plotted as a function of reaction time for a CH_3CN solution of **1**$^{2+}$ (c = 3.6·10^{-5} M) with varying equivalents of catechol (see SI for details). The lower concentration relative to the NMR experiment leads to a

massive deceleration of the reaction, being now completed in 500 h (30000 min, Figure 6).

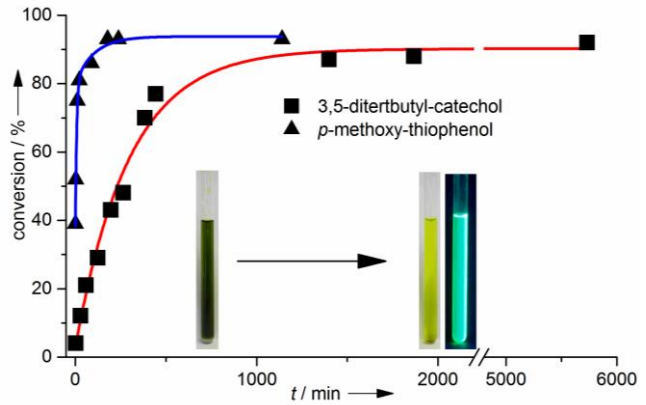

Figure 5. Conversion vs. time plots (see SI for details) from NMR experiments on the PCET reaction of $\mathbf{1}^{2+}$ (c = 17.8·10^{-3} M) with 1.2 equivalents of 3,5-ditertbutyl-catechol (red curve) or 2.0 equivalents of *p*-methoxy-thiophenol (blue curve, c = 8.5·10^{-3} M); both in CD_3CN.

Additional experiments show that the rate is highly solvent dependent, being much faster in DMSO, where it is completed in 1500 min. Subsequently the catechol concentration was steadily increased to obtain information about the reaction order with respect to $\mathbf{1}^{2+}$ (Figure 6). The reaction with 100 eq. of catechol is ca. 10 times faster than with 10 eq. After an initial period of ca. 800 min, the log(I_N) vs. time plot follows a linear relationship (see SI), in line with a first order kinetics with respect to $\mathbf{1}^{2+}$, with a reaction rate of 5.9·10^{-4} s^{-1}. In the initial period the rate is slower, indicating an autocatalytic effect of one of the products. Most likely, the formation of an hydrogen-bonded complex between the catechol and (**1**+2H)$^{2+}$ (see below and Figure 7) weakens the catechol O-H bonds and thereby supports the PCET process. Experiments with different concentrations of $\mathbf{1}^{2+}$ and a constant excess of 100 eq. catechol are in line with a pseudo-first order kinetics (similar half-value times $t_{1/2}$, see SI).

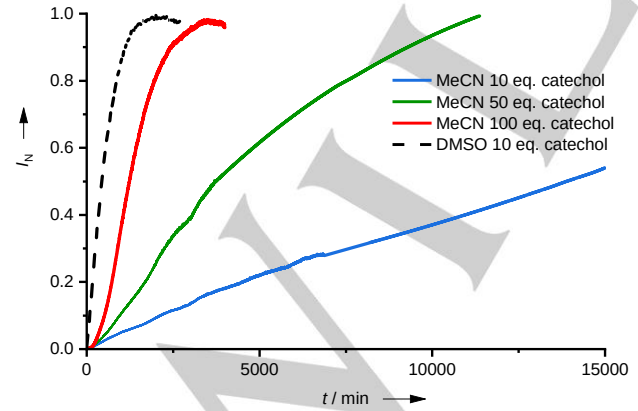

Figure 6. Normalized fluorescence intensity (I_N) as a function of reaction time for PCET reaction between 3,5-ditertbutyl-catechol and $\mathbf{1}^{2+}$ (c = 3.6·10^{-5} M).

UV/Vis spectra, recorded immediately after mixing the two reagents together, give no evidence for the formation of a complex between $\mathbf{1}^{2+}$ and catechol, even for a large excess of catechol (see SI). In additional experiments, solutions of the PCET product (**1**+2H)$^{2+}$ are titrated with the catechol reagent (Figure 7). The band at 417 nm in the UV/Vis spectrum of (**1**+2H)$^{2+}$ starts to shift and split into two components for addition of more than ca. 50 eq. of catechol (Figure 7). Upon addition of 400 eq. of catechol, a large UV/Vis band appears at 356 nm and a small band at ca. 445 nm. The maximum of fluorescence shifts to 405 nm (λ_{ex} = 356 nm). These results indicate the formation of a hydrogen-bonded complex, in which the two unprotonated guanidino groups in (**1**+2H)$^{2+}$ act as hydrogen-bond acceptor and the OH groups of the catechol as hydrogen-bond donor. Hence a simple kinetic analysis is only possible in a certain concentration regime.

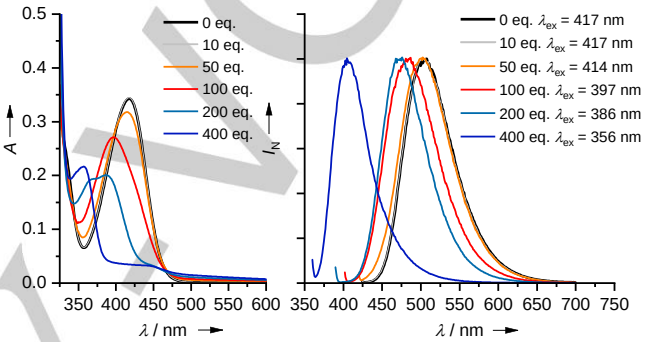

Figure 7. Changes in the absorption (left) and emission (right) spectra of (**1**+2H)$^{2+}$ (c = 3.76·10^{-5} M) upon addition of 3,5-ditertbutyl-catechol in CH_3CN solution.

In summary, we report herein a rational approach to new PCET reagents with redox-state dependent fluorescence, merging the concepts of cross-conjugated cruciform chromophores with the strategy of imposing redox-activity and Brønsted basicity on aromatic compounds by substitution with guanidino groups. The new GFA cruciform (GFA = Guanidino-Functionalized Aromatics) is stable in all relevant protonation and oxidation states. It is fluorescent in its reduced (and protonated) state, and the quantum yield is highly temperature-sensitive. On the other hand, it is fluorescence-silent in its oxidized state. Its PCET reactivity was shown by the examples of oxidative thiol coupling and catechol oxidation experiments. Model PCET reactions with 3,5-ditertbutyl-catechol, using the redox-state dependent fluorescence to follow the conversion, show that the reaction rate increases with solvent polarity and concentration and argue for simultaneous proton and electron transfer. These experiments illuminate the strength of the fluorescence sensing, but also the limitations arising from the formation of hydrogen-bonded complexes at high substrate concentrations. Purely organic PCET reagents showing comparable redox-state dependent fluorescence were hardly known up to date. Based on previous work by our group on redox-active GFAs, the established strategies for tuning the electrooptic properties of cross-conjugated cruciforms [20] can now be used to develop a whole family of such compounds.

Keywords: proton-coupled electron transfer • guanidine • oxidation• fluorescence • redox-active organic compounds

[1] a) I. Siewert, *Chem. Eur. J.* **2015**, *21*, 15078–15091; b) A. Migliore, N. F. Polizzi, M. J. Therien, D. N. Beratan, *Chem. Rev.* **2014**, *114*, 3381–3465; c) S. Y. Reece, D. G. Nocera, *Annu. Rev. Biochem.* **2009**, *78*, 673–699; d) M. H. V. Huynh, T. J. Meyer, *Chem. Rev.* **2007**, *107*, 5004–5064; e) S. Y. Reece, J. M. Hodgkiss, J. Stubbe, D. G. Nocera, *Phil. Trans. R. Soc. B* **2006**, *361*, 1351–1364.

[2] H. G. Yayla, R. R. Knowles, *Synlett* **2014**, *25*, 2819–2826.

[3] E. C. Gentry, R. R. Knowles, *Acc. Chem. Res.* **2016**, *49*, 1546–1556.

[4] M. Kumar, A. Sinha, J. S. Francisco, *Acc. Chem. Res.* **2016**, *49*, 877–883.

[5] J. M. Mayer, *Annu. Rev. Phys. Chem.* **2004**, *55*, 363–390.

[6] a) S. Hammes-Schiffer, A. V. Soudackov, *J. Phys. Chem. B* **2008**, *112*, 14108–14123; b) S. Hammes-Schiffer, *J. Am. Chem. Soc.* **2010**, *132*, 18127–18140.

[7] C. Costentin, M. Robert, J.-M. Savéant, *Chem. Rev.* **2008**, *108*, 2145–2179.

[8] J. S. Kretchmer, T. F. Miller III, *Inorg. Chem.* **2016**, *55*, 1022–1031.

[9] N. Elgrishi, B. D. McCarthy, E. S. Rountree, J. L. Dempsey, *ACS Catal.* **2016**, *6*, 3644–3659.

[10] a) J. M. Mayer, *Acc. Chem. Res.* **2011**, *44*, 36–46; b) C. T. Saouma, J. M. Mayer, *Chem. Sci.* **2014**, *5*, 21–31; c) N. Dietl, M. Schlangen, H. Schwarz, *Angew. Chem.* 124, 5638–5650; *Angew. Chem. Int. Ed.* **2012**, *51*, 5544–5555.

[11] A. Gansäuer, L. Shi, M. Otte, I. Huth, A. Rosales, I. Sancho-Sanz, N. M. Padial, J. E. Oltra, *Top. Curr. Chem.* **2012**, *320*, 93–120.

[12] M. Salamone, M. Bietti, *Acc. Chem. Res.* **2015**, *48*, 2895–2903.

[13] a) O. S. Wenger, *Acc. Chem. Res.* **2013**, *46*, 1517–1526; b) A. Pannwitz, O. S. Wenger, *Dalton Trans.* **2018**, DOI: 10.1039/c8dt04373f.

[14] I. A. Kieffer, R. J. Allen, J. L. Fernandez, J. L. Deobald, B. L. Thompson, J. D. Wimpenny, Z. M. Heiden, *Angew. Chem.* **2018**, *130*, 3435–3438; *Angew. Chem. Int. Ed.* **2018**, *57*, 3377–3380.

[15] a) H.-J. Himmel, *Z. Anorg. Allg. Chem*. **2013**, *639*, 1940–1952; b) B. Eberle, O. Hübner, A. Ziesak, E. Kaifer, H.-J. Himmel, *Chem. Eur. J.* **2015**, *21,* 8578–8590.

[16] H.-J. Himmel, *Synlett* **2018**, 29, 1957–1977.

[17] U. Wild, S. Federle, A. Wagner, E. Kaifer, H.-J. Himmel, *Chem. Eur. J.* **2016**, *22*, 11971–11976.

[18] U. Wild, F. Schön, H.-J. Himmel, *Angew. Chem.* **2017**, *129*, 16630–16633; *Angew. Chem. Int. Ed.* **2017**,*56*, 16410–16413.

[19] a) J. Piera, J.-E. Bäckvall, *Angew. Chem.* **2008**, *120*, 3558–3576; *Angew. Chem. Int. Ed.* **2008**, *47*, 3506–3523; b) X.-Q. Zhu, C.-H. Wang, H. Lang, *J. Org. Chem*. **2010**, *75*, 7240–7257; c) S. Lerch, L.-N. Unkel, P. Wienefeld, M. Brasholz, *Synlett* **2014**, *25*, 2673–2680; d) S. Lerch, L.-N. Unkel, M. Brasholz, *Angew. Chem.* **2014**, *126*, 6676–6680; *Angew. Chem. Int. Ed.* **2014**, *53*, 6558–6562; e) A. E. Wendlandt, S. S. Stahl, *Angew. Chem.* **2015**, *127*, 14848–14868; *Angew. Chem. Int. Ed.* **2015**, *54*, 14638–14658; f) M. T. Huynh, C. W. Anson, A. C. Cavell, S. S. Stahl, S. Hammes-Schiffer, *J. Am. Chem. Soc.* **2016**, *138*, 15903–15910.

[20] See for example: A. J. Zuccero, P. L. Mcgrier, U. H. F. Bunz, *Acc. Chem. Res.* **2010**, *43*, 397–408.

[21] I. M. Kolthoff, M. K. Chantooni, Jr., *J. Chem. Eng. Data* **1999**, *44*, 124-29.

[22] H.-s. Kim, T. D. Chung, H. Kim, *J. Electroanal. Chem.*, **2001**, *498*, 209-15.

[23] See recent work on a related (non-fluorescent) redox-active tetrakisguanidine: U. Wild, O. Hübner, L. Greb, M. Enders, E. Kaifer, H.-J. Himmel, *Eur. J. Org. Chem.* **2018**, 5910–5915.

10.1002/chem.201900268

WILEY-VCH

Entry for the Table of Contents

COMMUNICATION

A novel PCET reagent with redox-state depending fluorescence was developed by merging the concept of cross-conjugated cruciform chromophores with the concept of imposing redox-activity and high Brønsted basicity on aromatics by substitution with guanidino groups.

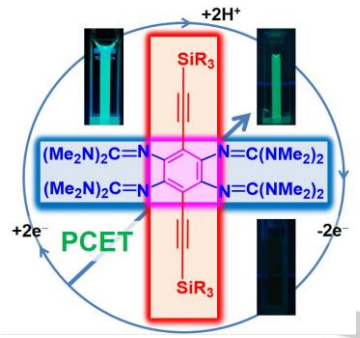

*C. Wagner, O. Hübner, E. Kaifer, H.-J. Himmel**

Page No. – Page No.

Probing the Proton-Coupled Electron Transfer Reactivity of a Cross-Conjugated Cruciform Chromophore by Redox-State Dependent Fluorescence